Al-Azhar Bulletin of Science

Volume 24 | Issue 1 Article 16

6-1-2013

Section: Earth science

EVALUATION OF THE SINKHOLE HAZARD AT ALISSAWIAH SOUTH OF QURAYAT GOVERNORATE, JOUF REGION, KINGDOM OF SAUDI ARABIA

ABDULLAH A. SABTAN
Engineering and environmental geology department, faculty of earth Sciences, king Abdul-Aziz University, Jeddah, KSA.

LAILA A. FAYED
Geology Department, Faculty of science, Cairo University, Egypt.

HUSSAM A. KHIYAMI
Geohazards department, Saudi Geological Survey, Jeddah, KSA.

How to Cite This Article

SABTAN, ABDULLAH A.; FAYED, LAILA A.; and KHIYAMI, HUSSAM A. (2013) "EVALUATION OF THE SINKHOLE HAZARD AT ALISSAWIAH SOUTH OF QURAYAT GOVERNORATE, JOUF REGION, KINGDOM OF SAUDI ARABIA," *Al-Azhar Bulletin of Science*: Vol. 24: Iss. 1, Article 16.
DOI: https://doi.org/10.21608/absb.2013.6572

Al-Azhar Bull. Sci. Vol. 24, No. 1 (June.): pp. 1-16, 2013.

EVALUATION OF THE SINKHOLE HAZARD AT ALISSAWIAH SOUTH OF QURAYAT GOVERNORATE, JOUF REGION, KINGDOM OF SAUDI ARABIA

ABDULLAH A. SABTAN[1], LAILA A. FAYED[2], and HUSSAM A. KHIYAMI[3]

1. *Engineering and environmental geology department, faculty of earth Sciences, king Abdul-Aziz University, Jeddah, KSA.* Email: asabtan2009@gmail.com
2. Geology Department, Faculty of science, Cairo University, Egypt. Email: Layla_Fayed@yahoo.co.uk
3. Geohazards department, Saudi Geological Survey, Jeddah, KSA. Email: khiyami.ha@sgs.org.sa

Abstract

Different types of sinkholes have been recognized in the Kingdom of Saudi Arabia (KSA). These sinkholes are of various sizes, shapes and occur at different depths. Their presence may create direct risk to the infrastructural facilities. Other types of sinkholes appeared mostly in a rural areas. This paper deals with the evaluation of the geological factors leading to the formation of sinkholes and their impacts on the land developments in Al Issawiah area, Al Jouf region in the northern part of the KSA. It promotes idea of karst region in the KSA, which represents a real geological hazard that affects a large area. The bases of the methodology take into account the description, interpretation and analysis of the fundamental geological information to determine the features related to karst formation. In addition, the vertical extent of the sinkholes as well as the subsurface layering and groundwater aquifer characteristics are explored by different geophysical techniques (electrical resistivity and gravity methods). On the other hand, applying the also drilling program is used to understand the subsurface stratigraphy and the geotechnical characteristics of the subsurface sediments that are affected by the formation of sinkholes. Finally, establish a hazard zonation map is prepared by using Geographic Information System (GIS) for the areas that are potentially susceptible to sinkholes.

The field investigations and measurements enable the authors for the detection of two collapsible sinkholes in the study area (about 200 km^2 on a scale of 1:50,000).

Key words: Aquifer, geotechnical, gravity, karst, resistivity, risk, Sinkhole, stratigraphy.

1. Introduction

Different authors have studied the formation of karst features. For instance, Davies and Lord (1981), investigated the effect of cavities in the Dammam and Rus formations (limestone) in the city of Al Khobar. Jado and Johnson (1984), reported two large solution cavities in the Dammam dome. Vaslet et al. (1988), investigated a crevasse formed by solution action in Al Kharj area. Al Saafin et al. (1989), examined the geomorphology and groundwater recharge in the karstic terrain of the As Summan Plateau in the Umm er Radhuma Formation, central Saudi Arabia. The present study deals with:

(i) The conditions that lead to the formation of caves in Al Issawia area, Jouf Region, KSA.

(ii) The factors that generate cave collapse and the creation of sinkholes

The main objectives of this study are the investigation of the karst features that will be achieved by available topographic, geomorphologic, geologic and structural maps, with the utilizing satellite images. The idea is to determine whether the sinkholes are located on a well defined rock structures together with design and execution of the geophysical program, in order to understand the subsurface extent of the sinkholes. This is expected to help in exploring the target areas. Design and execution of the drilling program provides a basis for a better understanding of the subsurface conditions.

Location Of The Study Area

Issawiah is located at the north western part of the KSA which belongs administratively to Al-Jouf region, about 110 kilometers south of Qurayat governorate and 35 km from Tabarjal (Figure1). The study area approximately covers about 200 km^2 and it is located between:

Latitudes N 30 ° 40 ′ **and N** 30 ° 50 ′

Longitudes E 38 ° 00 ′ **and E** 38 ° 10 ′

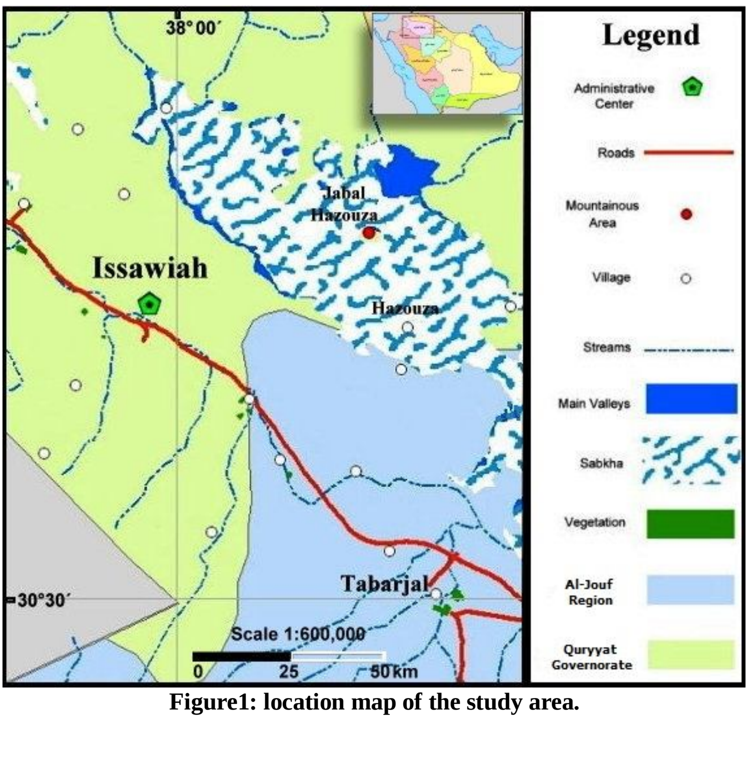

Figure1: location map of the study area.

The locations of the sinkholes are given as follows with their positions in figure 2**.** (See SH01 and SH02):

Sinkhole No.1: Located at **N** 30 ˚ 43′ 29.9″ and **E** 38 ˚ 05′ 59.9″

Sinkhole No.2: Located at **N** 30 ˚ 43′ 39.6″ and **E** 38 ˚ 04′ 05.1″

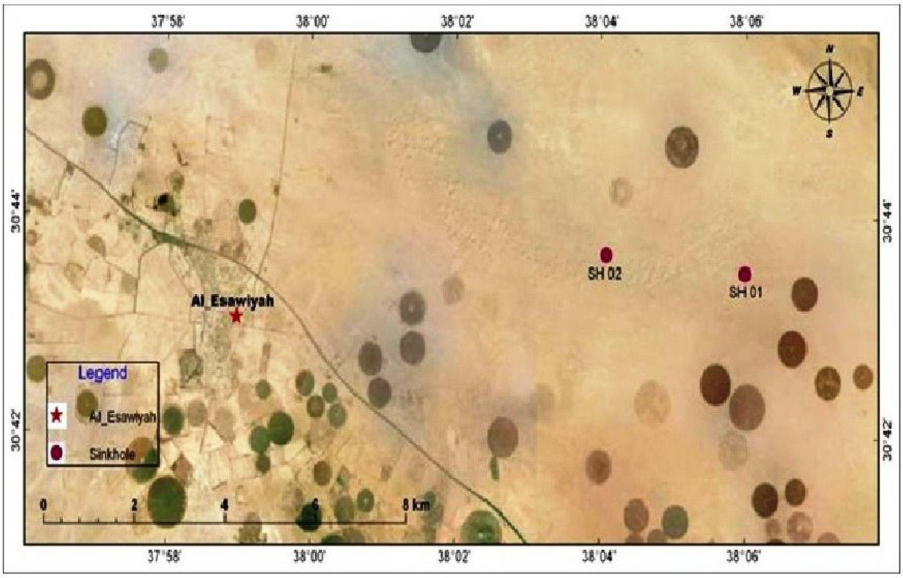

Figure 2: Landsat image showing the location of the sinkholes

2. Geology

Geological studies conducted on the formations in the northern region of KSA show that the phenomenon of karst originated for Geological period of Pliocene and Pleistocene (Quaternary) before the million years.The Arabian Peninsula had heavy rains until the pre-ten thousand years, which led to the creation of an environment for the growth of the karst phenomenon (Jado and Johnson, 1984)

Sirhan formation is composed of friable calcareous sandstone, limestone and shale that contains some of chert and claystone beds, with intercalation of basalt in some locations, which looks like small intermittent terraces (Wallace, 2000).The youngest Tertiary sedimentary rocks in the Wadi as Sirhan quadrangle are sandstone and interbedded limestone and chert of the Sirhan formation (Miocene to Pliocene), which is named from outcrops in the northern part of Wadi As Sirhan (Meissner et al., 1987).

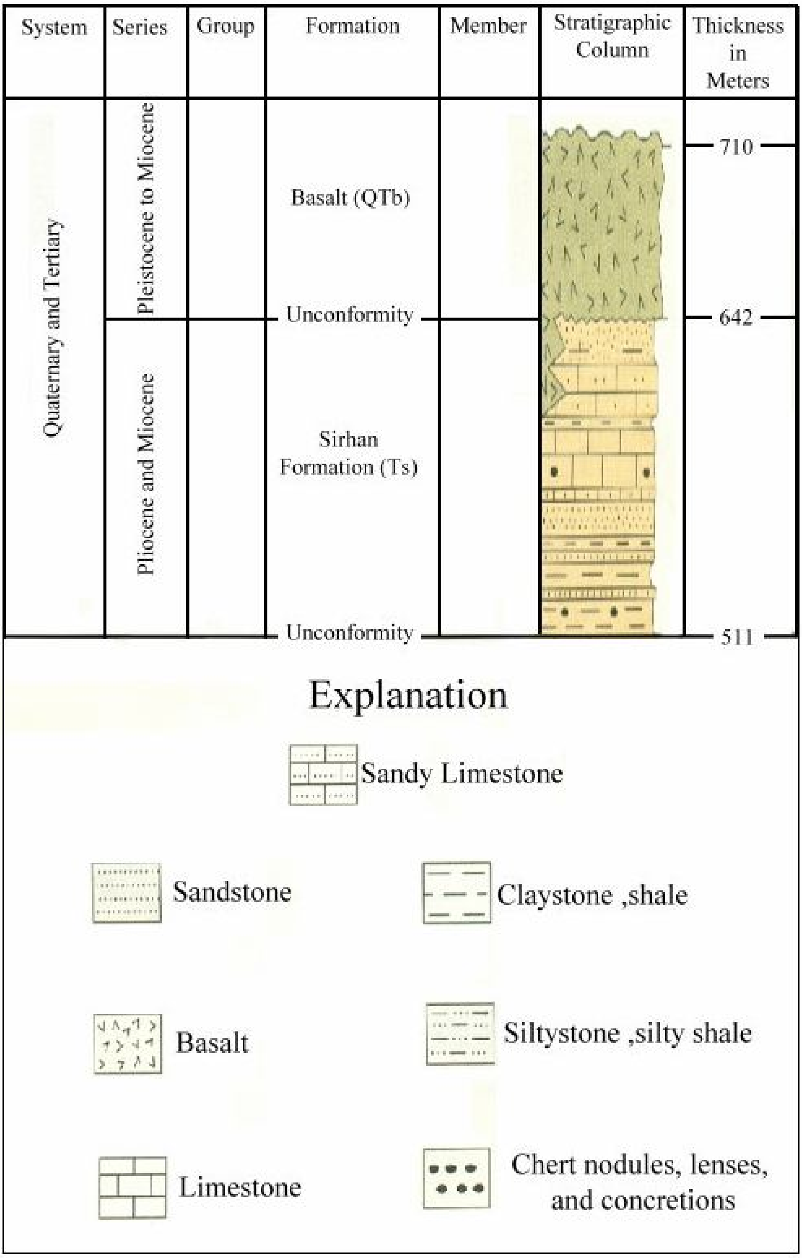

Figure 3: Lithostratigraphic column of rocks in the study area (Chester A. Wallace et al., 2000).

Figure 3 indicates the lithostratigraphic column that shows unconformities, basalt depths and sandstone as well as limestone layers.

Regional Geologic Structure

A part of the tectonic map of KSA and adjacent areas are compiled by Jonson, 1998 (Figure 5), where the normal faults of small separation are parallel to the general trend of the Wadi As Sirhan graben, but these extensional structures can be traced only for short distances. The Wadi As Sirhan graben extends in the western part of the Sirhan-Turaif basin and extends towards the north-west of Wadi As Sirhan quadrangle, and extends northward to the Jordanian terretories.

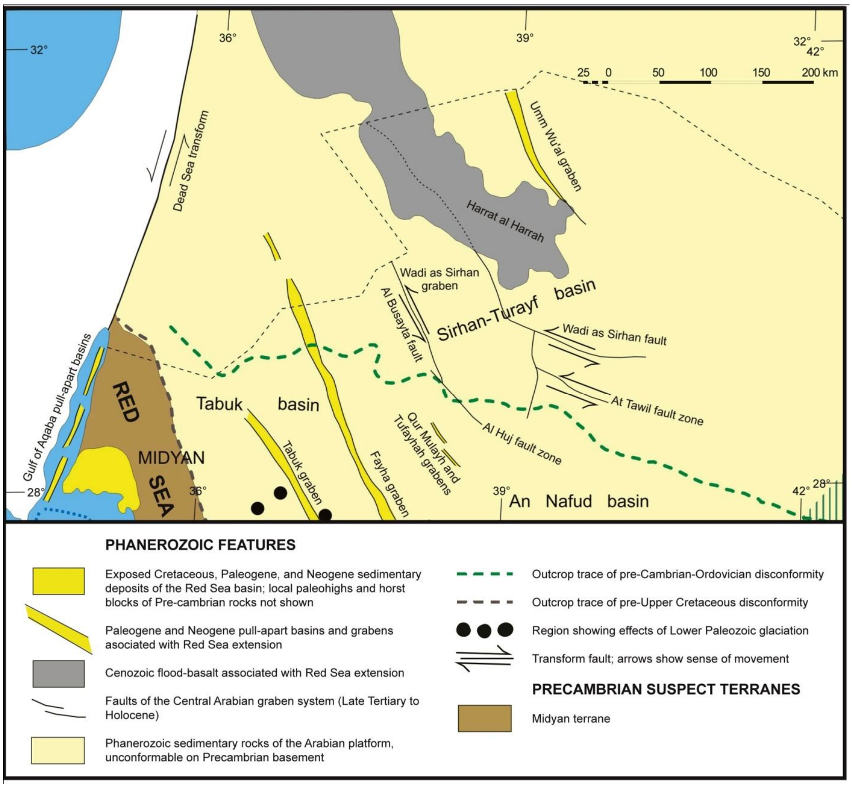

Figure 4: Part of the tectonic map of Saudi Arabia and adjacent area (Jonson P., 1998)

3. Hydrogeological Setting

In addition to The geological and geomorphological aspects, the hydrogeological factors play a distinctive role in the formation of sinkholes and their performances by time.

Local Hydrogeology

In the study area, since the aquifer is unconfined and the lithology is regionally heterogeneous, the zone of groundwater table fluctuation in the stratified layers in the stratigraphy become saturated and unsaturated in turn and this event leads to the weakness of the geological layers in this zone. Of course, since the subsurface is relatively heterogeneous regional weak zone distribution has a haphazard appearance, and accordingly some local areas will be subjected to sink earlier than others. This may lead to the occurrence of few sinkholes in the area, which is the case in the study area. Based on data obtained from the Table 1, the groundwater contour map, is given in Figure 6, in the form of equal piezometric levels. The groundwater flows from high piezometric level to low levels, and accordingly the regional flow trend is from northeast to southwest in the study area. Figure 6 implies that there is such continuous regional movement, which generates another mechanism for the sinkholes by washing the fine particles from weak locations and hence acceleration of the sinkhole events. Groundwater flow directions are shown by black arrows in Figure 5.

Table 1: Well locations, elevations and depths

Well No.	Depth (m)	Elevation (msl)	Location
B 2	25	546	N 30° 44′ 03.2″
			E 37° 56′ 10.2″
B 4	29	545	N 30° 44′ 14.4″
			E 37° 56′ 23.1″
B 7	22	543	N 30° 46′ 24.2″
			E 37° 53′ 09.4″
B 9	23	535	N 30° 45′ 28.0″
			E 38° 04′ 46.4″
B 11	33.6	545	N 30° 46′ 03.3″
			E 38° 01′ 20.2″
MW 1	30	550	N 30° 34′ 30.78″
			E 38° 06′ 34.26″
MW 2	35	547	N 30° 44′ 18.18″
			E 37° 55′ 47.76″
MW 3	40	542	N 30° 51′ 13.26″
			E 37° 51′ 56.22″
MW 5	60	668	N 31° 00′ 1.20″
			E 38° 11′ 3.48″

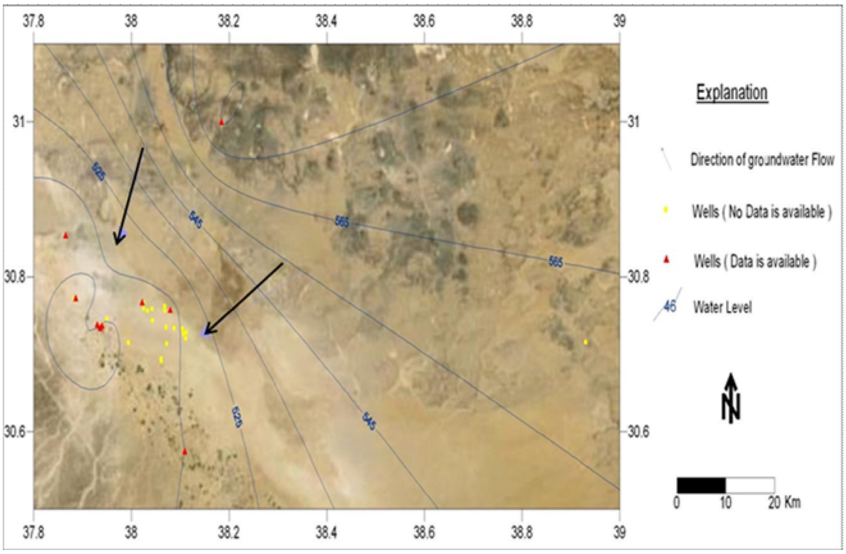

Figure 5: Ground water contour map

The location of each well is indicated in figure 6. It is possible to infer from the comparative location of the wells, that some of them are very close to each other, which may give rise to interferences. Such interferences lead to the speedy groundwater level falls around the wells, which may also trigger the sinkhole generation.

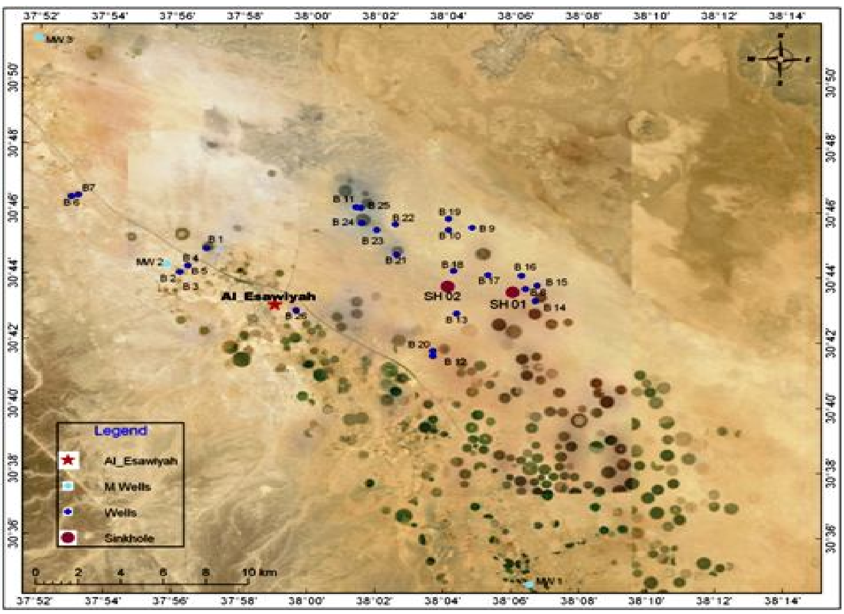

Figure 7: Wells location map

Water Quality

The general features of groundwater quality within the study area are given in Table 2 after the analyses of three samples, which are referred to as F2, F13 and F15, respectively.

Table 2: Chemical composition of water samples

Water Sample concentration / Parameter	Sample 1 (F2)	Sample 2 (F13)	Sample 3 (F15)
Ca (mg/l)	128.9	154.3	137.5
Mg (mg/l)	61	81.7	68.6
Na (mg/l)	396.2	488	404
K (mg/l)	29	35.3	17.7
Cl (mg/l)	762	1046	756
HCO3 (mg/l)	175	148	146
TDS (mg/l)	1980	2590	2090
pH	7.1	7	7.13
Temperature	33.2	33	33
Density	1	1	1
Pe	4	4	4

Based on obtained data (table 2), the PHREEQC (Version 2) program Issued by U. S. Geological survey, is applied for processing the results, following results shown (3, 4, and 5) for each sample, respectively.

PHREEQC software program allows the concentration of an element to be adjusted to obtain equilibrium (or a specified saturation index or gas partial pressure) with a specified phase. Solution compositions can be specified with a variety of concentration units (.Parkhurst, D.L., 1995). It is shown that all samples, are unsaturated with the minerals, Aragonite – calcite – dolomite and halite. This leads from (Saturation index, SI). The CO_2 is a partial pressure of carbon dioxide.The saturation indix (SI) is determined by using the amount of the precipitated or dissolved calcite.

$$\mathbf{SI = \log RS}$$

Where RS shows the relative saturation, which is the ratio of calcium carbonate activity product (K_{AP}) to calcium carbonate solubility product (K_{SP}).

Pe value is the phase name of the saturation index, which is adjusted to achieve specified saturation index with the specified phase.

The total dissolved solid (TDS) average value is in the range of 1900 to 2000 ppm (Table 2), the all SI values are with minus sign (Tables 3, 4 and 5). Which indicates that the groundwater is still having a potential power to erode or dissolve the limestone further and enlarge the existing caves or create new ones?

Table 3: Results of water sample (1)

Water Sample	Sample 1 (F2)		
Minerals	SI	Log K_{AP}	Log K_{SP}
Anhydrite ($CaSo_4$)	-	-	-
Aragonite ($CaCo_3$)	-0.16	-8.55	-8.39
Calcite ($CaCo_3$)	-0.02	-8.55	-8.53
Carbon Dioxide (Co_2)	-1.77	-19.91	-18.14
Dolomite ($CaMg(Co_3)_2$)	-1.25	-5.84	-17.28
Gypsum ($CaSo_4$:$2H_2o$)	-	-	-
Halite (NaCl)	-5.19	-3.59	-1.6

Table 4: Results of water sample (2)

Water Sample	Sample 2 (F13)		
Minerals	**SI**	**Log KAP**	**Log KSP**
Anhydrite (CaSo4)	-	-	-
Aragonite (CaCo3)	-0.29	-8.69	-8.39
Calcite (CaCo3)	-0.16	-8.69	-8.53
Carbon Dioxide (Co2)	-1.76	-19.9	-18.14
Dolomite (CaMg(Co3)2)	-0.17	-17.44	-17.27
Gypsum (CaSo4:2H2o)	-	-	-
Halite (NaCl)	-4.97	-3.37	-1.6

Table 5: Results of water sample (3)

Water Sample	Sample 3 (F15)		
Minerals	SI	Log K_{AP}	Log K_{SP}
Anhydrite ($CaSo_4$)	-	-	-
Aragonite ($CaCo_3$)	-0.22	-8.61	-8.39
Calcite ($CaCo_3$)	-0.08	-8.61	-8.53
Carbon Dioxide (Co_2)	-1.89	-20.03	-18.14
Dolomite ($CaMg(Co_3)_2$)	-0.05	-17.32	-17.27
Gypsum ($CaSo_4$:$2H_2o$)	-	-	-
Halite (NaCl)	-5.19	-3.59	-1.6

4. Geophysical Exploration

As part of the study includes, gravity, electrical resistivity traverses methods. These techniques were conducted around the sinkholes in order to determine the depth of the layer undergoing solution that has resulted in the collapses. The possible lateral extent of any nearby solution cavities was also investigated using these geophysical methods methods.

The Bouguer gravity anomaly around sinkhole 1 is shown as a slight gradient across the grid and therefore a first order (planar) trend was removed from the Bouguer grid to give the image in (Figure 8), which also employs a scale with a colour interval of 0.035 milligal.

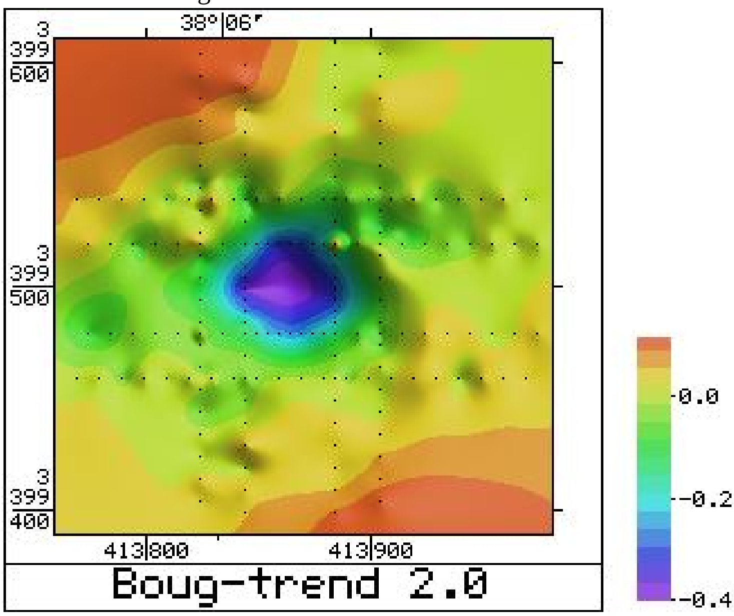

Figure 8: Bouguer gravity minus regional trend around sinkhole 1

An anomaly of about -0.1 milligal would be consistent with a substantial dry cavity, about 30 m wide and 20 m high at a depth of around 40 m. This is of course a very approximate estimation that gives some idea of the possible size of any cavity.

The resistivity inversions for profiles H6 and H7 were used to generate a series of horizontal resistivity slices at different depths, as shown in (Figure 9). The interpreted location of the collapse structure is shown superimposed on the slices. For the upper 3 levels, the hole is associated with high values as the fill is dry, but at 21 m and 40 m depths the low resistivities are due to saturated collapse material. At 70 m, depth the high resistivity basement is observed.

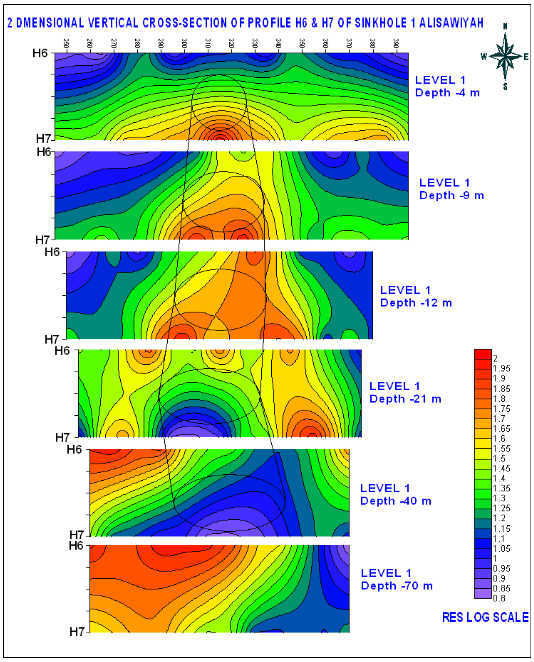

Figure 9: Horizontal resistivity slices at sinkhole 1

The relatively low resistivity zone (green) at about 40 m depth may be consistent with the low gravity trend that extends to the west of the cavity (Figure 8).

The Bouguer gravity anomaly for sinkhole 2 is shown in Figure 10, with a colour interval of 0.015 milligal. The locations of the gravity stations are also shown in this image.

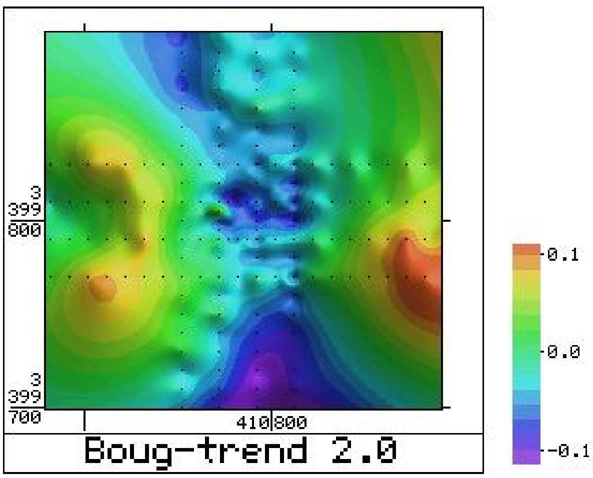

Figure 10: Bouguer gravity minus regional trend around sinkhole 2

The central anomaly is much less well defined than that at sinkhole 1, and has an amplitude less than 0.1 milligal.

The gravity data suggest that the cavity extends up to 30 m to the east of the surface collapse, with a general low trend in the gravity to the north and south (Figure 10). This may be due to a channel in the aquifer along which solution and cavities are occurring.

In this section (Figure 11), which lies to the north of the collapse, the underlying cavity zone at about 40 m depth, is well defined, with a width of about 80 m. The aquifer does not appear to be continuous at this depth, but there are two shallower low resistivity saturated zones at about 30 m depth, further to the right (east), that may be prone to solution cavities. These regions should perhaps be checked by drilling.

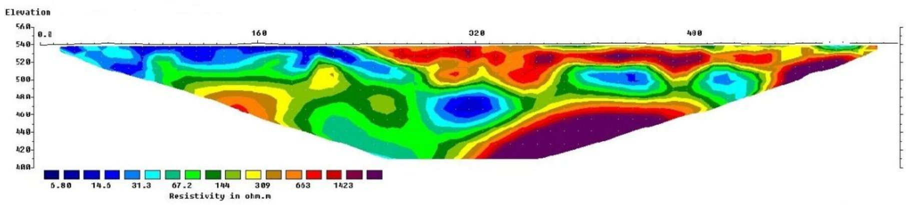

Figure 11: West-east resistivity section H3 at sinkhole 2

5. Geotechnical Investigation

GEOTECHNICAL INVESTIGATIONS ON SINKHOLE NO.1

Drilling

One hole (Table 6) were drilled close to Sinkhole 01, the hole was drilled vertically to depth of 100.7 m (SH01 – BH 01), until penetrating a reasonable distance in the Sirhan formation. Drill hole (SH01 – BH01) is located 37 m to the SE of the Sinkhole.

Table 6: Data of hole drilled close to Sinkhole 01

No.	Drill hole ID	Location		Total Depth (m)	Angle of drilling (*)	Elevation (m)
		Latitude	Longitude			
1	SH01 BH01	30 ° 43´ 30.3 "	38 ° 06´ 02.8 "	100.4	90	534

The rate of vertical drilling confirmed the horizontal geophysical resistivity slices for profiles H6 and H7(figure 9), with the collapsing material underneath the sinkhole at depths between 21 and 40 m.

Laboratory test results

The high RQD values indicate the low subsurface mechanical erosion. The fast rate of drilling in the borehole at several depths confirms the weak mechanical engineering characteristics (Table 7).

The mechanical properties of the rock core samples of SH01 BH01 are given in table 7. The uniaxial compressive strength (UCS) of the intact Sirhan formation limestone core samples ranges between 3.3 and 18.9 Mpa with an average value of 9.5 (Table 7).

The calculated tensile strength (TS) of Sirhan formation limestone ranges between 0.7 and 3.8 with an average value of 1.9 (Table 7).

Table 7: Mechanical properties of the Sirhan formation limestone (SH01-BH01)

SH01-BH01 (90 °)							
Test No.	**Sample No.**	**Depth (m)**	**Run (m)**	**Drilling Rate (min/m)**	**RQD (%)**	**UCS (Mpa)**	**TS (Mpa)**
1	BH1-1	25.40-26.90	1.5	15.0	9.0	3.3	0.7
2	BH1-2	28.40-29.90	1.5	15.0	40.0	5.1	1.0
3	BH1-3	34.40-35.90	1.5	20.0	23.0	3.8	0.8
4	BH1-4	53.90-55.30	1.4	23.0	62.0	18.5	3.7
5	BH1-5	61.40-62.90	1.5	15.0	38.0	18.9	3.8
6	BH1-6	67.40-68.90	1.5	22.0	40.0	6.3	1.3
7	BH1-7	79.40-80.90	1.5	15.0	73.0	16.1	3.2
8	BH1-8	85.40-86.90	1.5	13.0	79.0	7.8	1.6
9	BH1-9	98.90-100.4	1.5	15.0	40.0	5.7	1.1
Average						9.5	1.9

GEOTECHNICAL INVESTIGATIONS ON SINKHOLE NO.2

Drilling

one hole (Table 8) were drilled close to Sinkhole 02, the hole was drilled vertically to depth of 80 m (SH02 – BH 01), until penetrating a reasonable distance in the Sirhan formation. Drill hole (SH02 – BH01) is located 10.50 m to the SW of the Sinkhole.

Table 8: Data of hole drilled close to Sinkhole 02.

No.	**Drill hole ID**	**Location**		**Total Depth (m)**	**Angle of drilling (*)**	**Elevation (m)**
		Latitude	**Longitude**			
1	**SH02 BH01**	**30 ° 34´ 39.2 "**	**38 ° 04´ 04.7 "**	**80.0**	**90**	**536**

The rate of vertical drilling confirmed the geophysical resistivity section H3 (Figure 11), with the collapsing material underneath the sinkhole at depth 30 m, which is mentioned by geophysical survey as to be checked by drilling.

Laboratory test results

The Rock quality designation (RQD) values vary greatly with depth and occasionally showing very weak limestone with RQD values of 0% (Table 9), the low RQD values indicate the presence of an intense degree of fracturing and high subsurface mechanical erosion**.** The gradual erosion of these fractures by groundwater flow should have caused gradual subsidence, as is the case in a solution sinkhole. This shows the vulnerability to geological structures towards North Wes

The mechanical properties of the rock core samples of SH02 BH01 are given in table 9. The uniaxial compressive strength (UCS) of the intact Sirhan formation limestone core samples ranges between 5.7 and 8.3 Mpa with an average value of 7.1(Table 9).

The calculated tensile strength (TS) of Sirhan formation limestone ranges between 1.1and 1.7 with an average value of 1.4 (Table 9).

Table 9: Mechanical properties of the Sirhan formation limestone (SH02-BH01)

SH02-BH01 (90 °)							
Test No.	**Sample No.**	**Depth (m)**	**Run (m)**	**Drilling Rate (min/m)**	**RQD (%)**	**UCS (Mpa)**	**TS (Mpa)**
1	BH1-1	23.60-25.40	1.8	20.0	39.0	8.3	1.7
2	BH1-2	25.40-26.90	1.5	19.0	27.0	7.2	1.4
3	BH1-3	32.50-34.45	2.0	15.0	20.0	5.7	1.1
4	BH1-4	61.35-62.85	1.5	11.0	0.0	0.0	0.0
5	BH1-5	62.85-64.35	1.5	19.0	0.0	0.0	0.0
6	BH1-6	65.60-66.75	1.2	13.0	0.0	0.0	0.0
7	BH1-7	68.50-69.65	1.2	15.0	0.0	0.0	0.0
8	BH1-8	70.35-71.15	0.8	12.0	0.0	0.0	0.0
Average						7.1	1.4

6. **Conclusions**

Field work, chemical, geophysical and geotechnical studies showed the following significant points:

1. The geological settings of the studied locality including lithology, structural geology and geomorphology are suitable conditions for the creation of caves.
2. The sinkhole hazards were detected within limestone of the Sirhan formation.
3. One of the main reasons that are accelerated the general ground subsidence in the study area showed by the presence of rift or graben along the valley.
4. Two large-scale sinkholes were formed as the caves underneath were collapsed due to the scale of agricultural activities and the inadequate water management.
5. The obtained TDS and SI values indicated that more caves can be formed with time and some caves may collapse in the near future due to the excessive water pumping.

6. The present two sinkholes are limited to the zone within contour 540 above sea level, it is the same area that includes numerous and closely spaced water wells.
7. If the present wells pattern and the pumping rate continue in the area, then it is expected that more ground subsidence will occur in the near future.
8. Sinkhole No.01 is characterized by a layer of basaltic flow at the top, this strong layer has a sufficient tensile strength which allows the cave underneath to become larger than the one in Sinkhole No.02.
9. The limestone of Sirhan formation is highly cracked towards northwest of the study area, as indicated by the variations in Rock Quality Designation (RQD) values of the obtained core samples, when comparing Sinkhole No.1 and Sinkhole No.2.
10. The Sirhan formation is the main aquifer in the north western part of the Kingdom of Saudi Arabia. Accordingly, the active groundwater flows through the study area, thus enlarging the cracked rock and leading to larger cavities.
11. Sinkhole hazard zonation map (Figure 12) was delineated to classify the risk degree. The area that contains the present sinkholes, water wells and the extensive scale of agricultural fields within the north-west south-east trends structural control of the area, is ranked as the most risky part, and was recognized by red color. The area that is characterized by the presence of a large number of circular features was considered as a source of possible sinkholes in the future, and marked by the yellow color. The limestone of the Sirhan formation is very deep in the southwestern and northeastern parts and hence, marked by green color indicating a safe area.

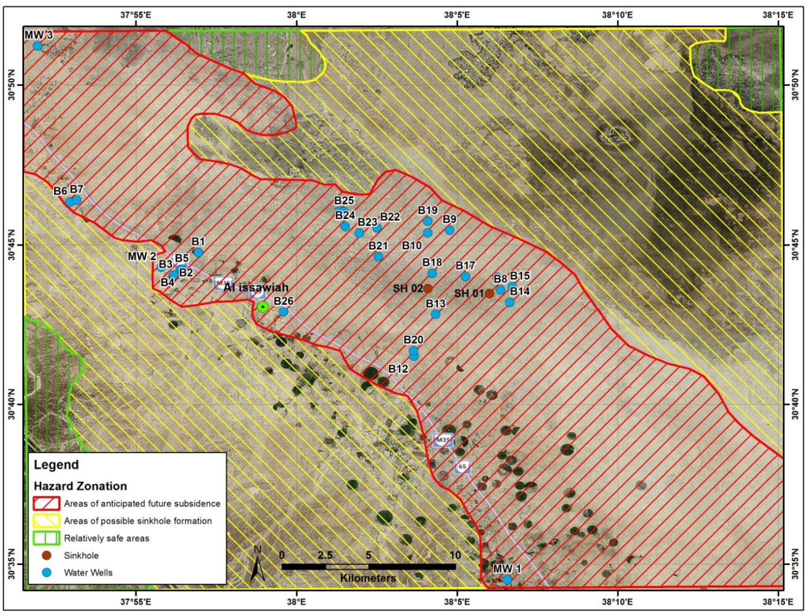

Figure 12: Hazard zonation map of the study area

References

1. Al Saafin, A.K., Bader, T.A., Shehata, W.M., Hoetzl, H., Wohnlich, J.G., and Zoetl, J., 1989, Groundwater recharge in an arid karst area in Saudi Arabia: 28th International Geologic Congress, Washington D.C., July 1989 (Also in Selected Papers on Hydrogeology from the 28th International Geologic Congress, E. S. Simpson and J. M. Sharp, Jr. (eds.), Verlag Heinz Heise, Hanover, Germany, p. 29-41, 1990).

2. Butler D.K. 1984. Microgravimetric and gravity gradient techniques for detection of subsurface cavities. Geophysics 41, 1016-1130.

3. Cooper S.S. and Ballard R.F. 1988. Geophysical exploration for cavity detection in karst terrain. American Society of Civil Engineers Geotechnical Special Publication 14, 25-39.

4. Davies, J. A. and Lord, J. A., 1981, The effects of cavities in limestone on the construction of a high rise building in Al Khobar, Saudi Arabia: Proc. Symp. on Geotechnical Problems in Saudi Arabia, v. Ia, 16 p.

5. ISRM, 1985, Suggested method for determining point load strength: Inter. Jour. Rock Mech. & Min. Sci., April 1985.

6. Jado, A. R. and Johnson, D. H., 1984, Solution caverns in the Dammam dome, Dhahran, Saudi Arabia: Arabian Jour. Sci. Engng., v. 8, no. 1, p. 69–73.

7. Johnson, Peter R. 1419 A.H. 1998 A.D. Tectonic map of saudi arabia and adjacent areas. Ministry of Petroleum and Mineral Resources, Deputy ministry for mineral resources technical report, USGS-TR-98-3 (IR-948).

8. Kleywegt R.J. and Enslin J.F. 1973. The application of the gravity method to the problem Africa. In Proceedings of Symposium on Sinkholes and Subsidence, International Association of Engineering Geologists: Hannover, 301-315.

9. Meissner, C.R., Jr., Riddler, G.P., van Eck, Marcel, Aspinall, N.C., Farasani, A.M., and Dini, S.M., 1987, preliminary geologic map of Turayf quadrangle, sheet 31C, and part of the An Nabk quadrangle, sheet 31B, Kingdom of Saudi Arabia: Saudi Arabian Deputy Ministry of Mineral Resources Open-File Report USGS-OF-07-3, 29 p., scale 1:250,000.

10. Parkhurst, D.L., 1995, User’s guide to PHREEQC--A computer program for speciation, reaction-path, advective-transport, and inverse geochemical calculations: U.S. Geological Survey Water-Resources Investigations Report 95-4227, 143 p.

11. Sadiq, A. M. and Nasir, S. J., 2002, Middle Pleistocene karst evolution in the State of Qatar, Arabian Gulf: Jour. Of Cave and Karst Studies, v. 64, no. 2, p. 132-139.

12. Shehata, W., Roobol J. M., Stewart, I., Khiyami, H., Al Khammash, A., Sayed, S., Tarabolsi, Y., and Al Ahmadi, K., 2007. Evaluation of A subsidence hazard in the Al Khafji area. Confidintial report Saudi Geological Survey.

13. Vaslet, D., Al Muallem, M. S., Madah, S. S., and Shorbaji, H., 1988, Preliminary technical investigation of a crevasse opened at Al Kharj end of February 1988: Ministry of Petroleum and Minerals Report, BRGM-JED-IR-88-1, 10p.

14. Wallace, C. A., Dini, S. M., and Al-Farasani, A. A., 2000. Geologic map of the Wadi as Sirhan quadrangle, sheet 30C, Kingdom of Saudi Arabia: Saudi Geological Survey Geoscience Map GM – 127C, scale 1:250,000.

15. Wilson W.L. and Beck B.F. 1988. Evaluating sinkhole hazard in mantled karst terrane. American Society of Civil Engineers Geotechnical Special Publication 14, 1-24.